Role of support in lean $DeNO_x$ catalysis

M. Piacentini, M. Maciejewski, T. Bürgi, and A. Baiker*

Swiss Federal Institute of Technology, ETH-Hönggerberg, Institute for Chemical and Bioengineering, CH-8093 Zurich, Switzerland

FTIR and pulse thermal analysis were applied to investigate catalysts containing Pt (1 wt%)/Ba (17 wt%) supported on γ-Al_2O_3, SiO_2 and ZrO_2. The aim was to learn how the support material affects the thermal stability of barium carbonate and its activity in the reaction to bulk $Ba(NO_3)_2$. The lower thermal stability of $BaCO_3$ in alumina supported samples was found to influence the formation of barium nitrate during the NO_x storage process. Quantification of $Ba(NO_3)_2$ formed during NO_x storage indicated that for alumina supported catalysts only ca. 30% of barium present in the sample is involved in the storage process. The low thermal stability found for alumina supported barium nitrite excludes its role in the formation of barium nitrate during interaction of NO_x with the catalyst at 300 °C. The studies indicate that γ-Al_2O_3 plays a major role in influencing the thermal stability of $BaCO_3$ and $Ba(NO_3)_2$. This finding seems to be relevant for the higher activity of γ-Al_2O_3-supported catalysts in NO_x storage reduction reactions.

KEY WORDS: Lean $DeNO_x$; $BaCO_3$; $Ba(NO_3)_2$ and $Ba(NO_2)_2$ thermal stability; pulse thermal analysis; role of the support in NO_x storage.

1. Introduction

Lean burn engines, working with an air/fuel ratio of about 22 (by weight), instead of the actual 14.6, have been developed mainly for improving fuel economy. Under these conditions conventional three ways catalysts (TWC) are not capable to reduce NO_x species due to lack of reducing agent in the exhaust gases. Among all the proposed solutions, the most promising are the NO_x storage catalysts: they trap NO_x when the engine works at lean conditions, and reduce adsorbed NO_x during a brief interval in which the engine runs at rich conditions.

NO_x storage catalysts for mixed lean conditions containing Al_2O_3-supported noble and alkaline earth metals were patented by Toyota [1] in 1994. In 1996, Takahashi *et al.* [2] proposed a storage mechanism in which NO is oxidized on Pt to NO_2, then stored as $Ba(NO_3)_2$ and subsequently reduced by HC activated on Pt sites. The primary role of Ba as storage compound was shown in [3–5], whereas some debate is still open about the kind and amount of Ba containing species active during NO_x storage. Applying TPD on activated catalysts Prinetto *et al.* [5] estimated that 50% of Ba is present as $BaCO_3$ which is subsequently decomposed by the formation of bulk $Ba(NO_3)_2$. Nova *et al.* [6] found that only 17% of Ba present in the catalyst is involved in the process of NO_x storage.

In situ FTIR studies were performed by several authors [5–11] showing the formation of both nitrite and nitrate species during storage of NO/O_2. Li *et al.* [12] stated that the higher the adsorption temperature, the higher is the concentration of nitrate compared to nitrite. Although several studies on selective catalytic reduction of NO with SiO_2, SiO_2/Al_2O_3 and ZrO_2-supported Pt catalysts were made [13–35], relatively little attention has been given so far to the influence of the support on NO_x storage behavior. It is not clear yet how the support material affects the stability and the chemical transformation of the Ba constituent. Higher dispersion and possible support interaction can lower the thermal stability of these components.

Here, we studied the influence of the support on the stability of $BaCO_3$ and on the formation of $Ba(NO_3)_2$ using thermoanalytical methods and DRIFT-spectroscopy. The relative amount of Ba species which is active in the storage of NO by formation of nitrate species is determined.

2. Experimental

Catalysts were prepared via wet impregnation of the supports using the procedure described in [11]. Commercial γ-Al_2O_3 (BET surface area 210 m^2/g), SiO_2 (200 m^2/g) and ZrO_2 (60 m^2/g) were impregnated with precursor solutions of $Pt(NH_3)_2(NO_2)_2$ and $Ba(CH_3COO)_2$ to a final loading of active metals of 1 wt% Pt and 17 wt% Ba. Catalysts were then dried at 80 °C for 12 h and finally calcined at 500 °C for 5 h.

XRD analysis was carried out on a Siemens D5000 powder X-ray diffractometer using the Cu -Kα radiation in step mode between 10 and 80° 2θ, with a step of 0.01° and 0.3 s $step^{-1}$.

Thermogravimetry (TG) combined with mass spectrometry (MS) was performed on a Netzsch STA 409 thermoanalyzer which was connected to a valve device enabling pulse thermal analysis (Pulse TA®). This set-up [36] allows the injection of controlled amounts (0.5–5 mL) of probe gas into a carrier gas stream flowing through the thermoanalyzer. The composition of the gas

* To whom correspondence should be addressed.
E-mail: baiker@tech.chem.ethz.ch

1022-5528/04/0700–0071/0 © 2004 Plenum Publishing Corporation

phase was monitored by a Balzers QMC 420 quadrupole mass spectrometer, which was connected to the thermoanalyzer by a heated (ca. 200 °C) stainless steel capillary. The experiments were carried out with 40,0 mg samples using 5 vol% O_2 in He or pure He when investigating the desorbed species from samples previously exposed to NO_x at 300 °C. In non-isothermal experiments the heating rate was 10 K/min.

DRIFT analysis was performed on a Bruker IFS 55 spectrometer. A Praying Mantis Diffuse Reflection attachment (DRA) coupled with a HVC-DRP2 reaction chamber (Harrick) was used. The composition of the gas phase was monitored by an Omnistar GSD 310 02 quadrupole mass spectrometer, which was connected to the DRIFT cell by a stainless steel capillary. Isothermal measurements were conducted at 300 °C while in non-isothermal experiments the heating rate was 6.5 K/min. Sample temperature was controlled with a thermocouple directly in contact with the catalyst powder. Spectra were recorded at a resolution of 4 cm^{-1} and bulk, KBr diluted, $BaCO_3$, $Ba(NO_3)_2$, $Ba(NO_2)_2$, $Ba(OH)_2$ and BaO were also measured and used as reference spectra.

3. Results and discussion

3.1. Thermal stability of barium carbonate

Temperature-programmed desorption experiments were performed with alumina, silica and zirconia-supported catalysts.

Evolution of CO_2 from catalysts stored at ambient conditions is shown in figure 1 for the Pt/Ba/Al_2O_3,

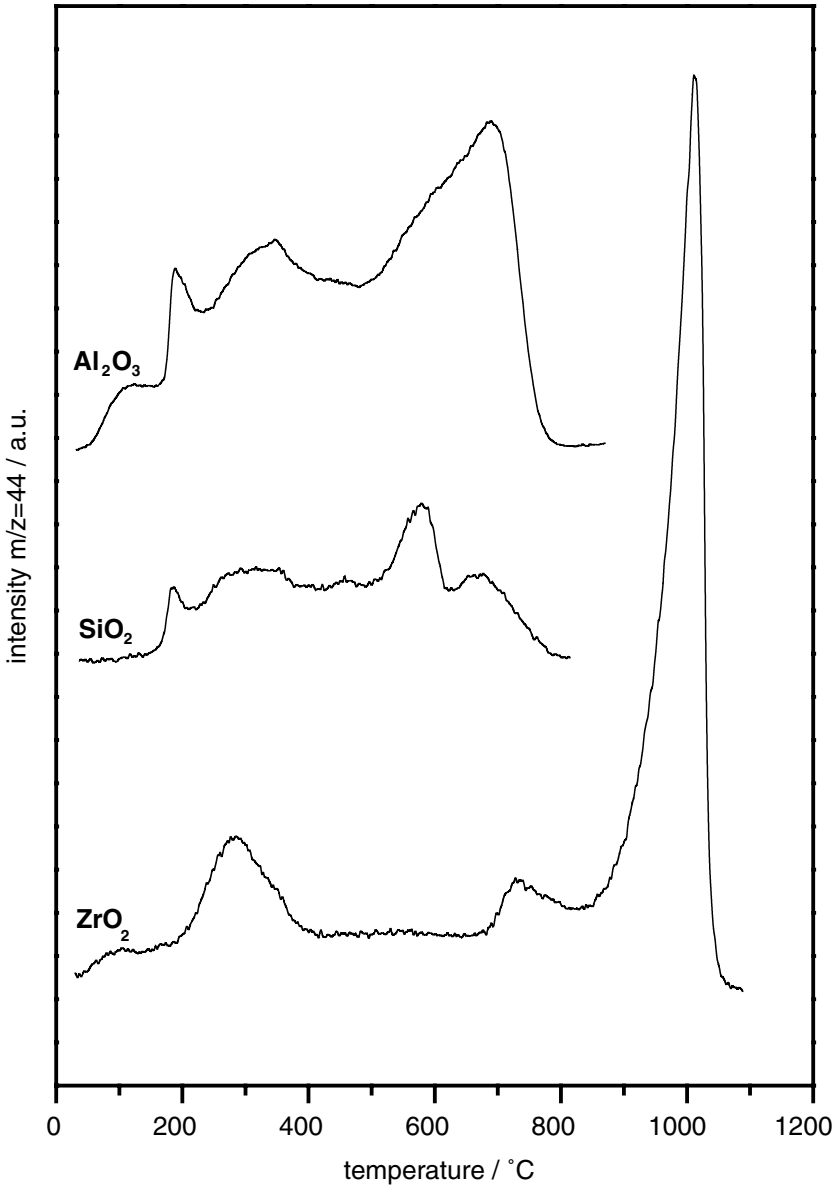

Figure 1. Evolution of CO_2 from catalysts containing Pt 1 wt% and Ba 17 wt% on different supports (Al_2O_3, SiO_2, ZrO_2) during TPD experiments carried out with TG-MS system.

$Pt/Ba/SiO_2$ and $Pt/Ba/ZrO_2$ samples. Four CO_2 desorption peaks can be observed for the Al_2O_3-supported sample appearing at ca. 100, 200, 350 and 680 °C, respectively. The first signal (around 100 °C), which appears with alumina and zirconia-supported catalysts, is due to weakly adsorbed monodentate and bidentate CO_2 [37] as confirmed by *in situ* DRIFT analysis (figure 2).

The sharp peak observed around 190–200 °C is very likely related to the combustion of adsorbed hydrocarbons, catalyzed by the presence of Pt. The disappearing of some peaks recorded by DRIFT related to C-H bonds starts around 150 –160 °C (figure 2). The peak at 350 °C is due to evolution of CO_2 species more strongly bound to Al_2O_3 [5,38] as confirmed by TPD with pure alumina (not shown) and CO_2 species stemming from decomposition of $BaCO_3$ which starts around 250–300 °C, as evidenced by DRIFT analysis. The rate of decomposition of $BaCO_3$ reaches its maximum around 680 °C, and rapidly decreases to zero at around 800 °C.

Note that the SiO_2-supported sample behaves similarly as the Al_2O_3-supported one till 500 °C (figure 1), at higher temperatures CO_2 evolves in two peaks (at 580 and 680 °C). This is probably related to the fact that for the alumina-supported sample XRD analysis had shown a considerable amount of crystalline $BaCO_3$, whereas in the SiO_2-supported sample the amount of crystalline $BaCO_3$ was neglectable and the major part of carbonates was present in amorphous form. The coexistence of crystalline and amorphous $BaCO_3$ led probably to its decomposition in two distinct temperature regions.

For ZrO_2-supported catalyst a prominent evolution of CO_2 occurs in the range of 820–1080 °C with a maximum at around 1000 °C. The decomposition of $BaCO_3$ is accompanied by the reaction of BaO with ZrO_2 resulting in formation of $BaZrO_3$, as corroborated by XRD analysis.

Results of DRIFT analysis of $Pt/Ba/Al_2O_3$ heated with a rate of 6.5 °C/min from 30–234 °C in 5% O_2/Ar are presented in figure 2.

Bands at 1660 cm^{-1} and those at 1530, 1370 cm^{-1} can be related to bidentate and monodentate CO_2. Bands at 2852 and 2931 cm^{-1} are assigned to C–H bonds originating from the presence of organic species which were adsorbed on the surface during exposure to air. The signal at 1660 cm^{-1} disappears completely at 190 °C. The two peaks characteristic to C–H bonds decrease in intensity above 160 °C. The simultaneously recorded mass spectrometric signal of $m/z = 32$ (not shown) confirmed the consumption of oxygen due to oxidation of adsorbed hydrocarbons resulting in formation of the CO_2 signal centered at ca. 200 °C (figure 1).

Comparison between Kubelka–Munk transformed DRIFT spectra of Ba/Al_2O_3 samples taken before and after the TPD at 300 °C (not reported) showed a decrease in intensity of bands due to $BaCO_3$ indicating the decomposition of carbonates. Decomposition of $BaCO_3$ species sets in between 200 and 300 °C.

In figure 3 a comparison of thermal stability between bulk $BaCO_3$ and $BaCO_3$ supported on Pt/Al_2O_3 is presented. Note that, on Pt/Al_2O_3, $BaCO_3$ starts to decompose at a much lower temperature than unsupported pure $BaCO_3$, which is stable till 800 °C. The same behavior was observed for the Pt/SiO_2-supported $BaCO_3$, whereas $BaCO_3$ on Pt/ZrO_2 starts to decompose at about 700 °C. Also in this case, $BaCO_3$ decomposition is completed much earlier than for bulk $BaCO_3$ (1080 and 1380 °C, respectively), because BaO formed during decomposition reacts immediately with ZrO_2

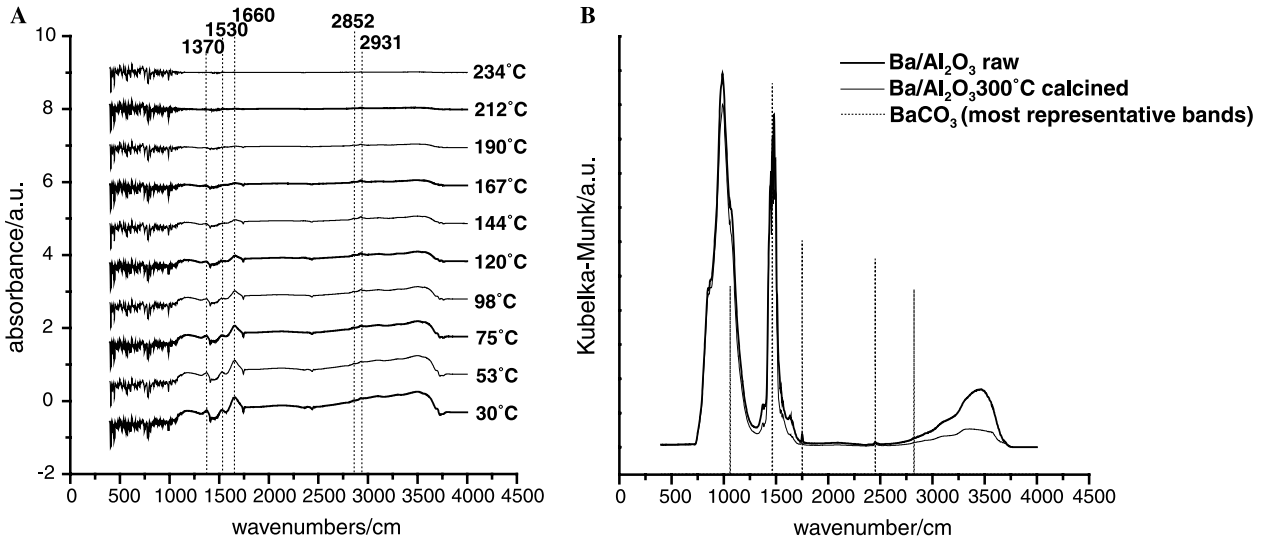

Figure 2. *In situ* DRIFT analysis of $Pt/Ba/Al_2O_3$. A. Spectra taken at different temperatures during TPD. Assignment of the bands: 1660 cm^{-1} bidentate CO_2, 1530 and 1370 cm^{-1} monodentate CO_2, and 2852 and 2931 cm^{-1} C-H bond. B. TPD of Ba/Al_2O_3. Note the decrease in the intensity of the Kubelka–Munk transformed signal characteristic for $BaCO_3$. Band 3000 – 3750 cm^{-1} is due to OH-groups and therefore is related to evolution of water.

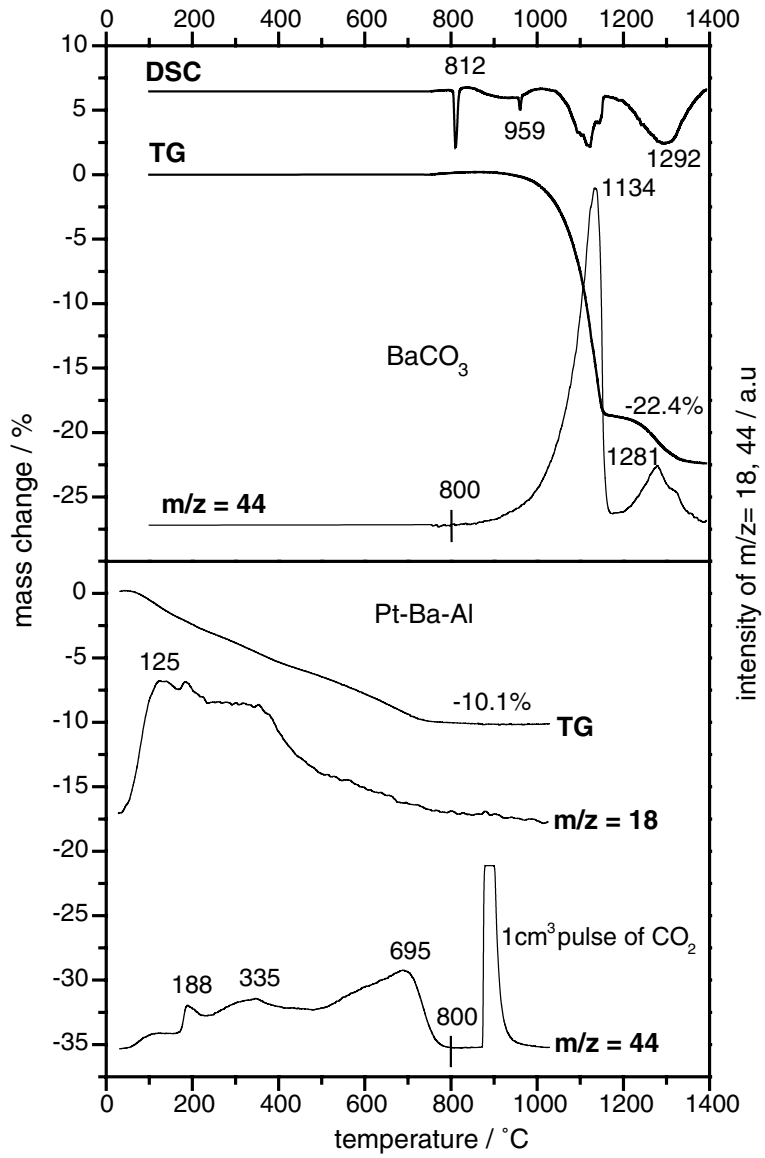

Figure 3. Comparison of decomposition of pure unsupported (top) and Pt/Al_2O_3 supported (bottom) $BaCO_3$ investigated by TA-MS. Changes of the mass (TG), thermal effects (DSC) and mass spectrometric signals of water ($m/z = 18$) and CO_2 ($m/z = 44$) are recorded during calcinations. The amount of CO_2 evolved from supported sample was quantified by PulseTA technique by injection of 1 cm^3 of CO_2 after decomposition.

forming $BaZrO_3$. The equilibrium of the decomposition reaction is consequently shifted and the decomposition is enhanced.

Table 1 lists the overall amount of CO_2 evolved from the raw catalysts during TPD experiments. The amount of CO_2 was determined using the PulseTA [36] technique by comparing the integral intensity of the CO_2 signal evolved during decomposition with the intensity of injected calibration pulses (1 cm^3) of CO_2. Quantitative analysis of Ba present as $BaCO_3$ based on the evolution of CO_2 during TPD experiments has been applied in another study [5]. In most cases, these analyses were performed with samples pretreated at 500 °C. Our results indicate that supported $BaCO_3$ starts to decompose at lower temperatures, around 250–300 °C. Thus it seems likely that previously reported $BaCO_3$ contents [5] are affected by the surprisingly low thermal stability of this material when supported on alumina and silica.

Table 1
CO_2 content in 40.00 mg samples of tested catalysts (in mg) determined by TA-MS

Support	Supported metal	Ba-doped supported metal	Ba-doped support
Al_2O_3	Pt/Al_2O_3	$Pt/Ba/Al_2O_3$	Ba/Al_2O_3
0.19	1.73	2.18	2.46
SiO_2	Pt/SiO_2	$Pt/Ba/SiO_2$	–
0.14	0.70	0.82	–
ZrO_2	Pt/ZrO_2	$Pt/Ba/ZrO_2$	–
0.29	0.25	2.23	–

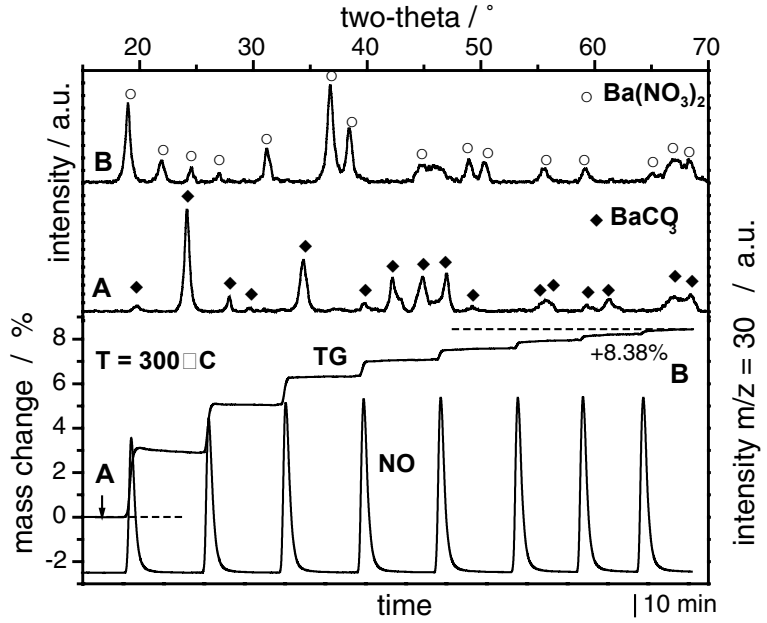

Figure 4. NO adsorption studied by PulseTA. Pulses of NO in 5% O_2/He were passed over alumina supported Pt/Ba catalyst at 300 °C resulting in formation of $Ba(NO_3)_2$ (B) from $BaCO_3$ (A).

3.2. Interaction of NO with the catalysts

The interaction of NO with the catalysts based on different supports was investigated using the PulseTA method. Pulses of NO (1 cm^3) in 5% O_2/He carrier gas were passed over the supported Pt/Ba catalysts at 300 °C. A representative experiment performed with $Pt/Ba/Al_2O_3$ is presented in figure 4. XRD analysis of the raw catalysts (figure 4, patterns A) revealed the presence of crystalline $BaCO_3$ in line with TEM analysis, which showed clusters of $BaCO_3$ up to 60 nm in size. Pulses of NO led to mass gain of the sample.

XRD analysis of the $Pt/Ba/Al_2O_3$ sample after exposure to NO pulses (figure 4, patterns B), corroborated the complete disappearance of $BaCO_3$ and the formation of crystalline $Ba(NO_3)_2$. $BaCO_3$ decomposition was also confirmed by evolution of CO_2 ($m/z = 44$) during the NO pulses (not shown).

The same experiments were performed with SiO_2 and ZrO_2-supported Pt/Ba (figure. 5(a)). Both samples showed a lower activity in NO_x storage reaction compared to the Al_2O_3-supported catalyst. This behavior indicates that less Ba containing species are active in NO storage in the silica and zirconia supported catalysts. It reveals that the support, beside the thermal stability, also affects the activity of $BaCO_3$ in the NO_x storage reaction. For $Pt/Ba/ZrO_2$ it can not be excluded that surface zirconium nitrate species can be formed [26].

Mass uptakes due to NO pulses (2 cm^3) at 300 °C in 5 % O_2/He are presented in figure. 5(b). Ba containing samples showed a much higher NO_x uptake, whereas some adsorption can be observed also on Pt/Al_2O_3 and Al_2O_3 samples. It is interesting to note that under the

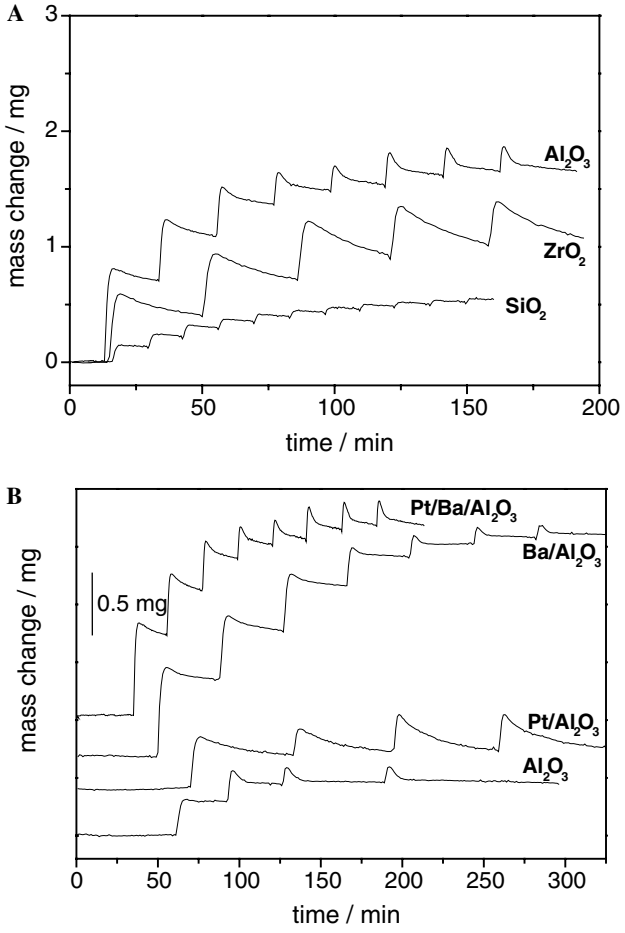

Figure 5. Pulses of NO in 5% O_2/He at 300 °C: A. Pt/Ba supported on Al_2O_3, SiO_2 and ZrO_2; B. Al_2O_3-supported samples: Pt/Ba, Ba, Pt and pure support.

applied experimental conditions platinum had no significant influence on the NO_x storage behavior of the barium containing catalysts. This could be attributed to the high temporary concentration of NO, which reached a maximum after injection of ca. 10,000 ppm. Additionally, due to the high surface area of the catalysts (ca.180 m^2/g) and relatively high reaction temperature (300 °C) we observed a high yield of NO oxidation, and thus NO_2 storage, even in the absence of Pt.

The catalysts after exposure to NO pulses in 5% O_2/He at 300 °C were analyzed by DRIFT-spectroscopy (figure 6(a) and 6(b)). Al_2O_3 and Pt/Al_2O_3 samples (figure 6(a)) contained carbonate species of various types (bands at 1300–1600 cm^{-1}), whereas Ba containing samples showed bands characteristic for bulk $BaCO_3$ (1:1 KBr diluted, figure 6(a) dotted lines). After NO + O_2 exposure at 300 °C, the Ba containing samples showed absorbance bands matching those of bulk $Ba(NO_3)_2$ (1:1 KBr diluted, figure 6(b) dotted lines) confirming the $BaCO_3 \rightarrow Ba(NO_3)_2$ conversion. Bands at 1343 and 1404 cm^{-1}, observed on Al_2O_3 and Pt/Al_2O_3 samples can be attributed to hyponitrite

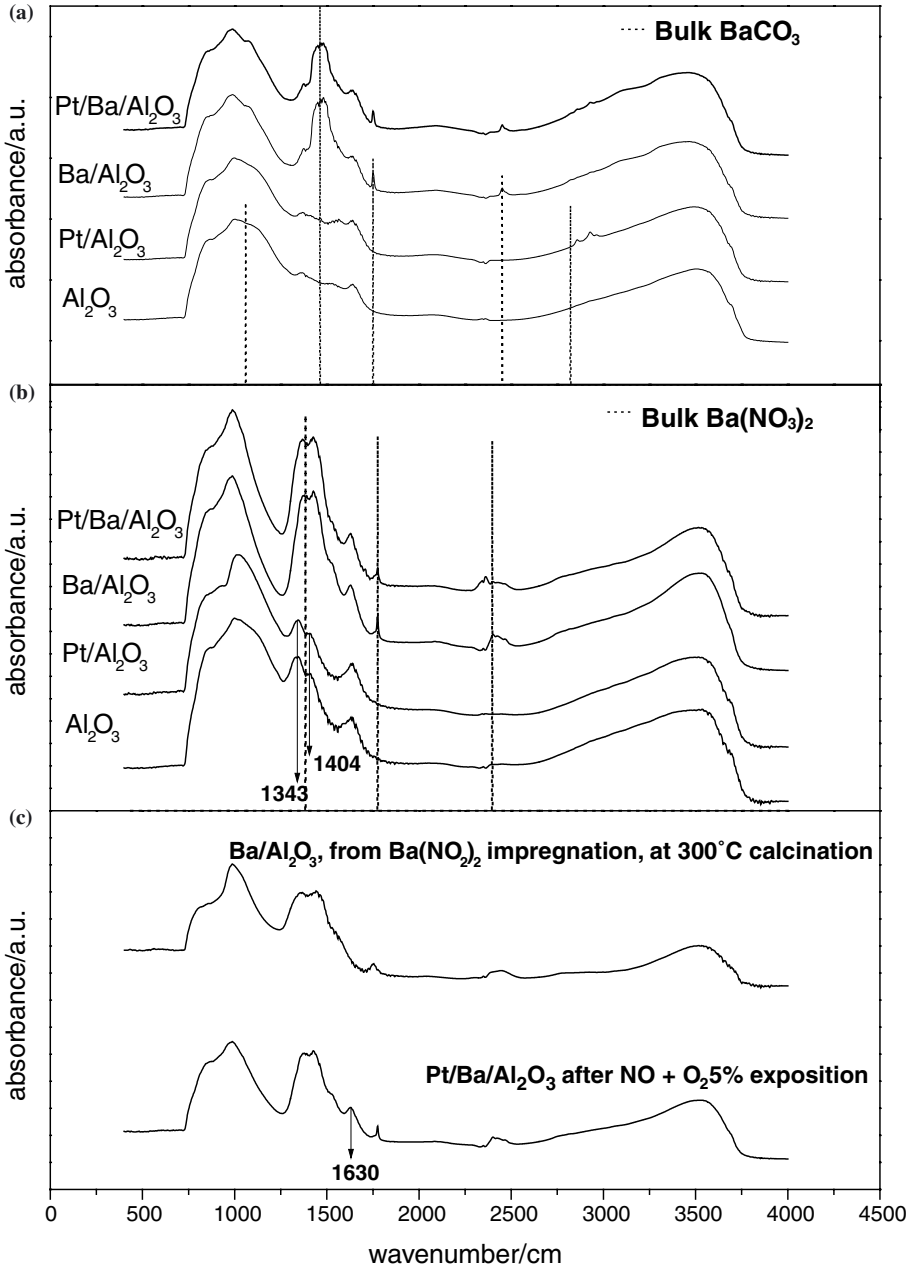

Figure 6. DRIFT analysis of $Pt/Ba/Al_2O_3$ catalyst at 35 °C: (a) Fresh samples; (b) Samples exposed to NO + 5% O_2/He at 300 °C: signals at 1343 cm^{-1} refer to hyponitrite (Al^+NO^-) and at 1404 cm^{-1} to nitrates species ($Al^+NO_3^-$) [8]; (c) DRIFT analysis of Al_2O_3 supported $Ba(NO_2)_2$ calcined in air at 300 °C and $Pt/Ba/Al_2O_3$ after exposure to NO + 5%O_2/He at 300 °C. Band at 1630 cm^{-1} refers to some carbonates adsorbed on the surface due to air exposure.

(Al^+NO^-) and to nitrates ($Al^+NO_3^-$) species, respectively [8]. A comparison between Al_2O_3-supported $Ba(NO_2)_2$ calcined in air at 300 ° and $Pt/Ba/Al_2O_3$ exposed to NO + O_2 at 300 °C is shown in figure 6(c). The close agreement of these two spectra indicates that nitrite is not stable at 300 °C, because in both samples only bands characteristic for nitrate species are present.

3.3. Thermal stability of NO adsorbed on different catalysts

Temperature-programmed desorption experiments were performed with alumina-, silica- and zirconia-supported catalysts after NO pulses at 300 °C.

Evolution of NO from $Pt/Ba/Al_2O_3$, $Pt/Ba/SiO_2$ and $Pt/Ba/ZrO_2$ is shown in figure 7(a). NO desorption from the Al_2O_3-supported sample occurs from 230 to 730 °C with maximum at 470 °C. Desorption of NO from the SiO_2-supported sample begins at 230 °C with a neglectable NO evolution. The main NO evolution occurs in the range 380 °C to 650 °C with a peak centered at around 530 °C. For the ZrO_2-supported catalyst a small evolution of NO is observed between 130 and 230 °C, before the main desorption peak smoothly starts. Around 500 °C a sharp and very intense peak shows up and NO evolution continues till ca. 800 °C.

Similar TPD experiments were also performed on Al_2O_3-supported Pt and Ba samples: mass spectrometric signals $m/z = 30$ (NO) and $m/z = 32$ (O_2) are presented in figure 7(b). Both Al_2O_3 and Pt/Al_2O_3 show a small NO evolution centered at about 130 and 160 °C, respectively. A shoulder at 350 °C for Al_2O_3 and at 300 °C for Pt/Al_2O_3 is not accompanied by the evolution of O_2, whereas in both cases the main NO desorption peaks (at 460 and 380 °C) are associated with O_2 evolution due to the decomposition of nitrate species (figure 7(b)). For both Ba containing samples, the evolution of NO alone is related to a small shoulder on the desorption curves between 350 and 400 °C, while again decomposition of $Ba(NO_3)_2$ is corroborated by evolution of NO and O_2 that reached a maximum at 550 °C for Ba/Al_2O_3 and at 490 °C for $Pt/Ba/Al_2O_3$. The amount of NO evolved from supported samples was quantified by PulseTA by injection of 1 cm^3 of NO after decomposition. Quantification of the NO resulting from the decomposition of $Ba(NO_3)_2$ allowed to estimate its amount formed during interaction of the sample with NO at 300 °C. This comparison revealed that only about 30% of the barium present in the sample was involved in the NO_x storage process. Some differences become apparent when comparing our results to previous investigations where the exposure of the catalysts to NO + O_2 was performed at 40 °C [5]. NO and O_2 evolution centered at around 550 – 600 °C was also observed but a distinct NO evolution around 300 °C was found only in case of low temperature exposure to NO + O_2. The authors attributed this evolution to decomposition of some nitrite species.

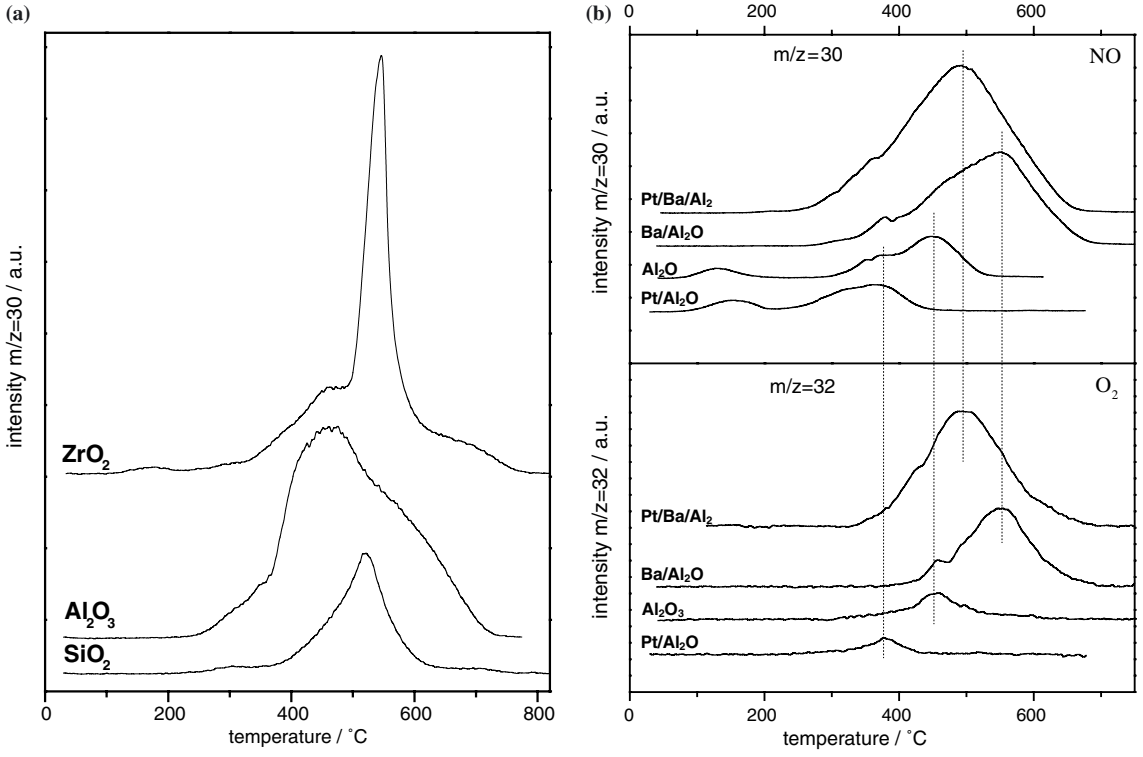

Figure 7. (a) Evolution of NO from Al_2O_3, SiO_2 and ZrO_2 supported Pt/Ba catalysts after prior adsorption at 300 °C in 5% O_2/He flow. (b) Evolution of NO and O_2 from alumina-supported catalysts after prior adsorption at 300 °C in 5% O_2/He flow.

To better understand these results, we prepared Al_2O_3-supported $Ba(NO_3)_2$ and $Ba(NO_2)_2$ via wet impregnation of the corresponding salts on alumina. Temperature-programmed decomposition/desorption experiments were performed with these two samples and with bulk $Ba(NO_3)_2$. In figure 8 (top) the decomposition/desorption curves of bulk $Ba(NO_3)_2$ (A), $Ba(NO_3)_2/Al_2O_3$ (B) and $Pt/Ba/Al_2O_3$ after NO + O_2 exposure at 300 °C (C) are presented. Note that nitrate formed during NO_x storage reaction on $Pt/Ba/Al_2O_3$ starts to decompose at a much lower temperature.

In figure 8 (bottom), mass spectrometric signals $m/z = 30$ (NO) and $m/z = 32$ (O_2) recorded during TPD of $Ba(NO_3)_2/Al_2O_3$ and $Ba(NO_2)_2/Al_2O_3$ are shown. Barium nitrite decomposition is characterized by a wide $m/z = 30$ peak centered at around 210 °C, while Ba nitrate starts decomposing at higher temperatures, with a NO peak centered at around 580 °C. Due to very low stability of supported $Ba(NO_2)_2$ (figure 8, bottom) which starts to decompose already below 100 °C, it is possible that the drying of the sample at 80 °C for 10 h resulted in the formation of traces of $Ba(NO_3)_2$ detected by DRIFT. DRIFT analysis of $Ba(NO_2)_2/Al_2O_3$ during TPD in the range of RT – 300 °C is shown in figure 9. As confirmed by the reference spectra of bulk $Ba(NO_2)_2$ and $Ba(NO_3)_2$, the characteristic band at 1250 cm^{-1} present in barium nitrite disappears during calcination. This confirms that NO evolution centered at 210 °C is related to $Ba(NO_2)_2$ decomposition.

The supported nitrate and nitrite species behave in a very different way compared to the corresponding bulk materials. Preparation and characterization of Al_2O_3-supported samples helped in determining the thermal stability of NO_x species on the catalysts. The low thermal stability of 17 wt% $Ba(NO_2)_2/Al_2O_3$ does rule out the possibility that at 300 °C some nitrites could be present among stored NO_x species on Al_2O_3-supported Pt and Ba catalysts.

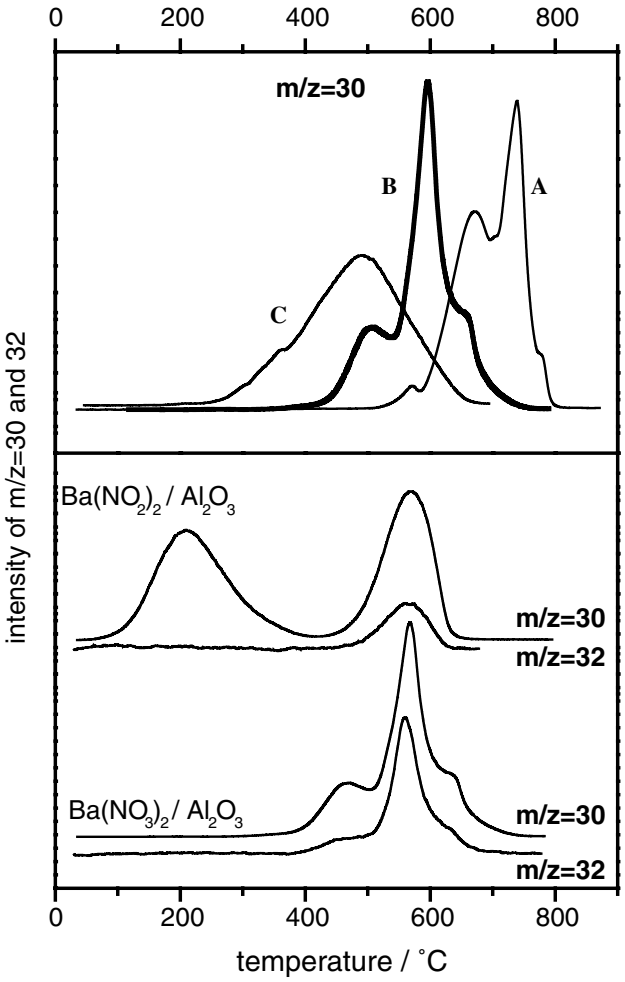

Figure 8. Thermal stability of $Ba(NO_3)_2$: (a) pure unsupported sample, (b) supported on Al_2O_3 prepared by wet impregnation, (c) supported on Pt/Al_2O_3 formed during injection of NO at 300 °C in 5% O_2/He (Top). Thermal stability of $Ba(NO_2)_2$ and $Ba(NO_3)_2$ supported on Al_2O_3 prepared by wet impregnation (Bottom).

4. Conclusions

The influence of the support on the stability of $BaCO_3$ and formation of $Ba(NO_3)_2$ was investigated by TPD, DRIFT-spectroscopy and Pulse Thermal Analysis on Pt and Ba containing catalysts supported on γ-Al_2O_3, SiO_2 and ZrO_2.

Experimental results confirmed the relationship between the stability of Ba containing species and their activity towards NO_x storage. The thermal stability of $BaCO_3$ was found to be distinctly influenced by the support which in turn affects the activity of $BaCO_3$ in NO_x storage reactions. The lower efficiency of SiO_2 and ZrO_2 supported samples for storing NO_x species can be related to their deficiency in active Ba sites, i.e. to the lower amount of thermally less stable $BaCO_3$ present in these systems.

DRIFT-spectroscopy revealed that $BaCO_3$ in $Pt/Ba/Al_2O_3$ starts decomposing between 250 and 300 °C, that is at much lower temperature than required for bulk $BaCO_3$ (ca. 800 °C).

Pt/Ba catalysts supported on γ-Al_2O_3, SiO_2 and ZrO_2 exposed to NO pulses in 5% O_2/He atmosphere showed complete disappearance of $BaCO_3$ and formation of crystalline $Ba(NO_3)_2$ as confirmed by XRD. Absence of Pt in Ba/Al_2O_3 sample did not influence significantly the NO_x storage. This behavior can be traced to the special conditions used in the pulse experiments, affording substantial production of NO_2, even in the absence of Pt. The presence of hyponitrite and nitrate species was confirmed on Pt/Al_2O_3 and Al_2O_3.

TPD experiments on pre-exposed catalysts confirmed that $Ba(NO_3)_2$ formed on $Pt/Ba/Al_2O_3$ is even less thermally stable than nitrate deposited through wet impregnation of Al_2O_3 with a $Ba(NO_3)_2$ solution. Both supported nitrates were less stable than bulk $Ba(NO_3)_2$. Quantification of the amount of NO evolved during

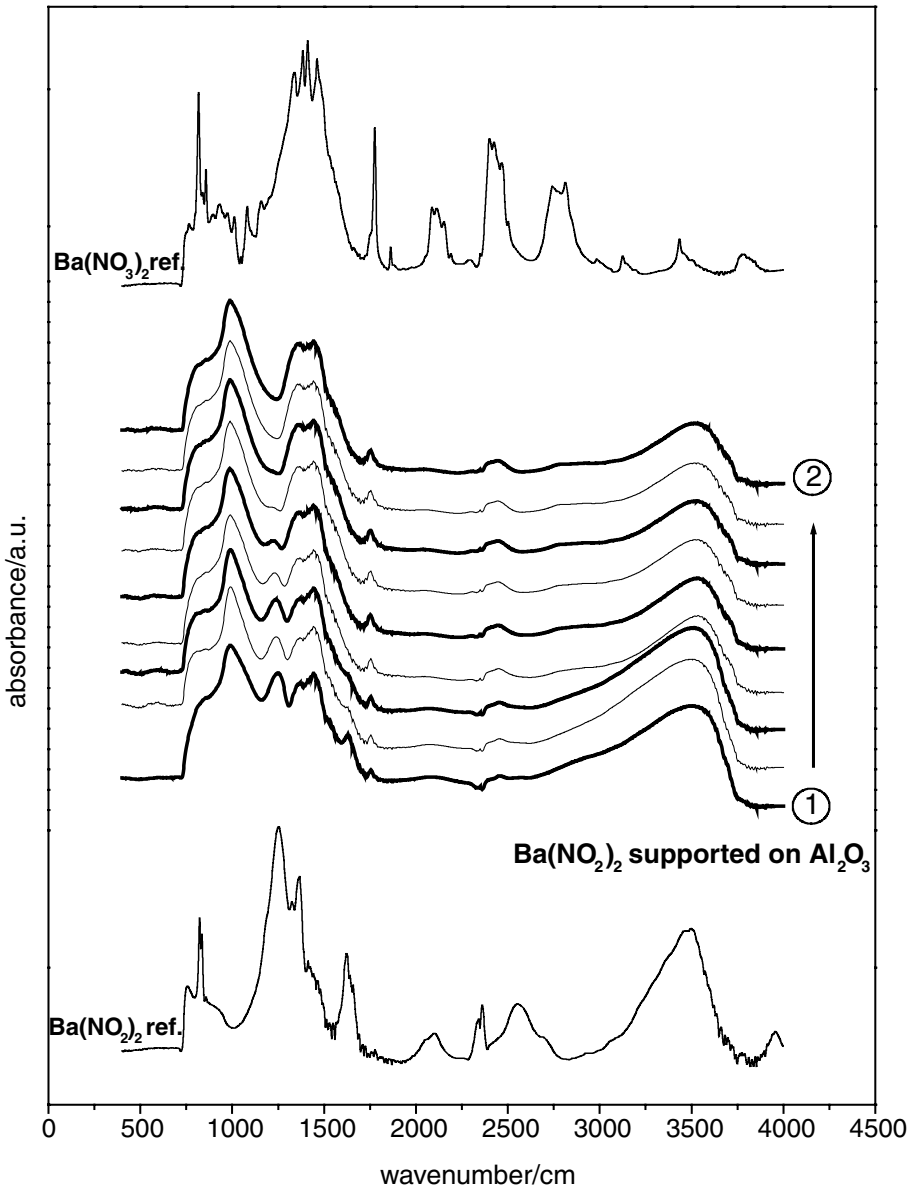

Figure 9. DRIFT analysis during TPD at different temperatures of $Ba(NO_2)_2$ supported on Al_2O_3 prepared by wet impregnation: 1. RT; 2. 300 °C, step 35 °C.

decomposition of barium nitrate formed during NO_x storage indicated that only 30% of the loaded Ba is involved in the NO_x storage process.

Finally, the low stability of supported barium nitrite, prepared by wet impregnation of alumina, questions whether formation of nitrates at 300 °C during NO_x storage proceeds via nitrite intermediates.

References

[1] S. Motohisa, S. Tadashi, M. Naoto, I. Satochi, K. Koichi, T. Toshiaki and T. Syuji, Catalyst and process for purifying exhaust gases, patent: EP0613714 (1994).
[2] N. Takahashi, H. Shinjoh, T. Iijima, T. Suzuki, K. Yamazaki, K. Yokota, H. Suzuki, N. Miyoshi, S. Matsumoto, T. Tanizawa, T. Tanaka, S. Tateishi and K. Kasahara, Catal.Today 27 (1996) 63.
[3] S. Matsumoto, Y. Ikeda, H. Suzuki, M. Ogai and N. Miyoshi, Appl. Catal. B 25 (2000) 115.
[4] S. Matsumoto, CatTech 4 (2000) 102.
[5] F. Prinetto, G. Ghiotti, I. Nova, L. Lietti, E. Tronconi and P. Forzatti, J. Phys. Chem. B 105 (2001) 12732.
[6] I. Nova, L. Castoldi, L. Lietti, E. Tronconi and P. Forzatti, Catal. Today 75 (2002) 431.
[7] C. Sedlmair, K. Seshan, A. Jentys and J.A. Lercher, J. Catal. 214 (2003) 308.
[8] B. Westerberg and E. Fridell, J. Mol. Catal. A-Chem. 165 (2001) 249.
[9] E. Fridell, M. Skoglundh, B. Westerberg, S. Johansson and G. Smedler, J. Catal. 183 (1999) 196.
[10] H. Mahzoul, J. F. Brilhac and P. Gilot, Appl. Catal. B 20 (1999) 47.
[11] L. Lietti, P. Forzatti, I. Nova and E. Tronconi, J. Catal. 204 (2001) 175.
[12] X. Li, M. Meng., P. Lin, Y. Fu, T. Hu, Y. Xie and J. Zhang, Top. Catal. 22 (2003) 111.
[13] R. Burch and P. J. Millington, Catal. Today 29 (1996) 37.

[14] Y.J. Mergler, A. vanAalst, J. vanDelft and B.E. Nieuwenhuys, J. Catal. 161 (1996) 310.
[15] K.L.R. Dinyar, K. Captain and M.D. Amiridis, Catal. Today 42 (1998) 93.
[16] R. Burch, A.A. Shestov and J.A. Sullivan, J. Catal. 186 (1999) 353.
[17] A.A. Shestov, R. Burch and J.A. Sullivan, J. Catal. 186 (1999) 362.
[18] R. Burch and J.A. Sullivan, J. Catal. 182 (1999) 489.
[19] C.P. Hwang and C.T. Yeh, J. Catal. 182 (1999) 48.
[20] F. Jayat, C. Lembacher, U. Schubert and J.A. Martens, Appl. Catal. B 21 (1999) 221.
[21] M.D.A. Dinyar and K. Captain, J. Catal. 194 (2000) 222.
[22] J.A. Sullivan, R. Burch and A.A. Shestov, Chem. Eng. Res. Des. 78 (2000) 947.
[23] J.L. Freysz, J. Saussey, J.C. Lavalley and P. Bourges, J. Catal. 197 (2001) 131.
[24] P. Denton, A. Giroir-Fendler, Y. Schuurman, H. Praliaud, C. Mirodatos and M. Primet, Appl. Catal. A 220 (2001) 141.
[25] E. Rocchini, M. Vicario, J. Llorca, C. de Leitenburg, G. Dolcetti and A. Trovarelli, J. Catal. 211 (2002) 407.
[26] K. Eguchi, T. Kondo, T. Hayashi and H. Arai, Appl. Catal. B 16 (1998) 69.
[27] K. Eguchi and T. Hayashi, Catal. Today 45 (1998) 109.
[28] M. Machida, A. Yoshii and T. Kijima, Int. J. Inorg. Mater. 2 (2000) 413.
[29] M. Machida, S. Ikeda, D. Kurogi and T. Kijima, Appl. Catal. B 35 (2001) 107.
[30] L.F. Liotta, A. Macaluso, G.E. Arena, M. Livi, G. Centi and G. Deganello, Catal. Today 75 (2002) 439.
[31] R. Mariscal, S. Rojas, A. Gomez-Cortes, G. Diaz, R. Perez and J.L.G. Fierro, Catal. Today 75 (2002) 385.
[32] S. Tuti, F. Pepe, D. Pietrogiacomi and V. Indovina, Catal. Today 75 (2002) 373.
[33] S. Kikuyama, I. Matsukuma, R. Kikuchi, K. Sasaki and K. Eguchi, Appl. Catal. A 226 (2002) 23.
[34] K. Hadjiivanov, V. Avreyska, D. Klissurski and T. Marinova, Langmuir 18 (2002) 1619.
[35] S. Tuti, F. Pepe, D. Pietrogiacomi and V. Indovina, Catal. Today 75 (2002) 373.
[36] M. Maciejewski, C.A. Müller, R. Tschan, W.D. Emmerich and A. Baiker, Thermochim. Acta 295 (1997) 167.
[37] G. Busca and V. Lorenzelli, Mater. Chem. 7 (1982) 89.
[38] J.B. Peri, Phys. Chem. 70 (1966) 3168.